JOURNAL OF APPLIED ELECTROCHEMISTRY 15 (1985) 365–377

*Determination of state-of-discharge of zinc–silver oxide button cells. II. Impedance measurements**

JEAN-PAUL RANDIN

ASULAB S.A., Passage Max-Meuron 6, 2001 Neuchâtel, Switzerland

Received 1 June 1984; revised 10 July 1984

The prediction of the state-of-discharge of numerous types of Zn–Ag_2O button cells from six international manufacturers has been investigated using the impedance technique over an extended frequency range. The frequency responses at various states-of-discharge are presented and it is shown that the changes in impedance which result from discharging provide several potential parameters for the state-of-discharge prediction. The complex impedance plot of the undischarged cells usually shows a fairly well-defined semicircle at high frequencies and a straight line with a slope between 40 and 50° at low frequencies. As discharge proceeds, the diameter of the semicircle increases and the overlap between the semicircle and the low-frequency straight line increases. The most attractive method would be to determine a parameter such as a characteristic relaxation frequency in the complex impedance plot. Unfortunately, no unambiguous characteristic parameter can be extracted due to the non-ideal shape of the impedance response at high frequencies. The determination of the diameter of the high-frequency semicircle has been faced with the same difficulties. The most reliable test was found to be the determination of either the phase of the impedance φ, or a corrected phase φ' taken from the high-frequency intercept. The proposed prediction is a 'go/no go' indication on the basis of one- or two-frequency measurements for φ or φ', respectively. The selection is made at 20–40% state-of-discharge. The charge withdrawn is negligibly small and the time of the test is between 1 and 100 s depending on the type of cell. A calibration is necessary for each cell dimension and each manufacturer. Some 10–16% of the types of cells investigated could not be selected successfully, mainly because of too large a dispersion of the electrical characteristics of the cells, especially for small newly developed types, and of the similarity of the φ and φ' values in the low and high state-of-discharge in the appropriate frequency range. The latter difficulty arises from the difference of the frequency response between the undischarged and the partly discharged cells occurring at high frequencies.

1. Introduction

A simple, rapid, reliable and nondestructive state-of-discharge indicator would be very helpful in predicting the residual capacity and warn the user about the need for an impending battery replacement. Existing battery test devices are not sufficiently accurate to predict the residual capacity in batteries with ease and confidence despite the many attempts reported in the literature for both primary and secondary batteries. A galvanostatic method has been proposed recently to determine the state-of-discharge of button size zinc–silver oxide cells [1]. The method is based on the slope or $\Delta E/\Delta t$ value of the potential vs time curve. Applications are limited to a 'go/no go' test with a selection at 50 ± 10% state-of-discharge. The charge withdrawn during the measurement is about 0.1% of the nominal capacity and a calibration is needed to determine the current level for each cell dimension, each manufacturer and possibly, each lot number.

The investigation of alternating current methods for the estimation of the state-of-discharge of Leclanché [2], alkaline Zn–MnO_2 [3–5], Zn–HgO [6], Li–SO_2 [7] primary cells and lead–acid [8, 9], nickel–cadmium [10] secondary cells has been reported recently. This

* This is the second of a series of papers dedicated to Professor Ernest Yeager on the ocasion of his 60th birthday.

0021–891X/85 $03.00 + .12

paper presents the results of a study aiming at the identification of a suitable, sensitive parameter based on some impedance characteristics and the development of a practical device capable of predicting with precision the residual capacity in Zn–Ag_2O button cells of unknown storage and discharge history.

2. Experimental details

The numerous sizes of low and high drain cells from six manufacturers throughout the world which were investigated are shown in Table 1. For each type of cell about 25 samples were used. Four lots of three to five samples each were discharged to 20, 40, 60 and 80% state-of-discharge, respectively. Five samples were kept undischarged. After the impedance measurements the resistive discharges were continued to determine the total capacity of each cell.

The discharges were performed on constant loads at ambient temperature. The resistive load was chosen for each size to give a complete exhaustion in about 30 days. Current drains varied between 9.7 μA for the smaller and 167 μA for the larger sizes. A cut-off voltage of 1.2 V was used.

At least 24 h were allowed to elapse after resistive loading before beginning ac impedance measurements in order to allow diffusional processes within the cell to become complete.

Table 1. Sizes of the cells investigated from six manufacturers (A–F) with the nominal capacity of each cell in mA h. (a) Low drain cells

Height (mm)	*Diameter* (mm)							
	6.8		*7.9*		*9.5*		*11.6*	
1.1	A	7	A	8				
1.4			A	15				
1.6	A	11	A	19	A	24		
	B	11	B	14				
2.1	A	15	A	20	A	30	A	48
	B	18	B	22			B	50
	C	16	C	20	C	33	C	48
	E	17	E	25	E	38		
2.6	A	24	A	29	A	52		
			B	30				
	C	20						
			E	32				
3.1			A	37			A	80
3.6			A	45				
4.2							F	113

Table 1. Sizes of the cells investigated from six manufacturers (A–F) with the nominal capacity of each cell in mA h. (b) High drain cells

Height (mm)	*Diameter* (mm)							
	6.8		*7.9*		*9.5*		*11.6*	
2.1			E	27			F	50
2.6			A	29				
			C	30				
			E	32	E	56		
3.6			F	45				
5.4							F	200

Note: In the text the dimensions of the cells are given as follows: diameter (mm) X height (mm), Manufacturer

Experiments were carried out to obtain the real and imaginary parts of the impedance of each cell poised at its rest potential over a range of frequencies from 1 mHz to 10 kHz. Generally, five measurements per frequency decade were performed. The equipment used was a frequency response analyser (FRA, Solartron Type 1174) controlled by a calculator (Hewlett-Packard 9825A) via HPIB (IEEE 488) Bus. An electrochemical interface (Solarton 1186) was used to control and measure the cell characteristics by superimposing the sine wave output of the FRA on an internally generated polarization voltage or current. Some experiments were performed galvanostatically at several dc current levels using the electrochemical interface to drive the cell. The alternating voltage superimposed was 2.5 mV rms. The experiments were carried out at room temperature.

3. Results

Typical complex impedance data at four states-of-discharge are shown in Fig. 1. The undischarged state showed a fairly well-defined semicircle at high frequencies and a straight line with a slope of between 40 and 50° C at low frequencies. As discharge proceeded, the diameter of the high-frequency semicircle, θ, increased (Fig. 2) and the separation between the latter and the straight line at low frequencies decreased significantly. At the same time the frequency at the maximum of the

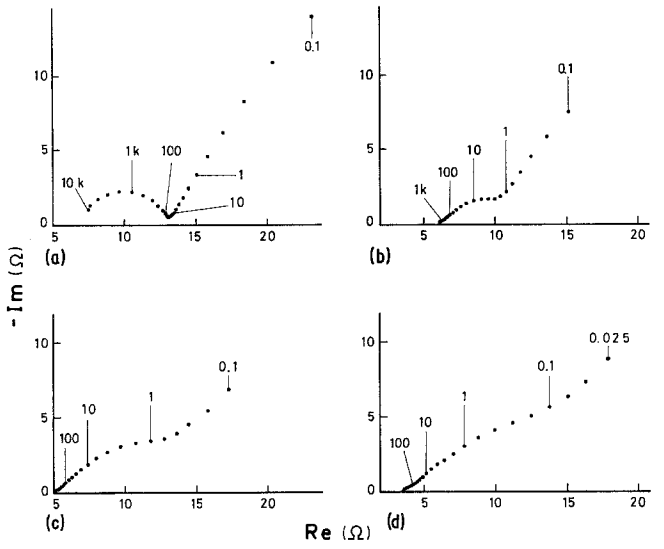

Fig. 1. Impedance data for a 11.6 mm × 2.1 mm (manufacturer A) low drain cell at (a) 0, (b) 20, (c) 40, and (d) 80% state-of-discharge at $i_{dc} = 0$. Number adjacent to points refers to frequency in Hz.

semicircle shifted toward lower frequencies. The high-frequency intercept with the real axis gives the value of the ohmic resistance. This change with the state-of-discharge varied too much from one type of cell to the other, and with the manufacturer, for a given size, to be used as a universal state-of-discharge indicator.

The use of the diameter of the high-frequency semicircle as a state-of-discharge indicator would require the determination of the impedance as a function of frequency starting from the higher frequency down to that at the minimum or inflexion point of the impedance plot. As a first approximation the value θ could be taken as the difference of the real component between the minimum or the inflexion point ($\mathrm{Re}_{(f_{min})}$) and the highest frequency ($\mathrm{Re}_{(f_\infty)}$). The frequency at the minimum or inflexion point, f_{min}, changed as a function of the state-of-discharge (Fig. 3).

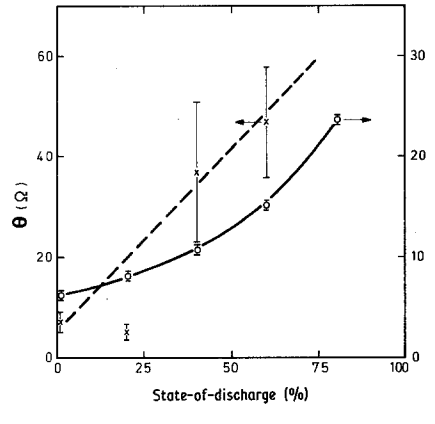

Fig. 2. Approximate diameter of the high-frequency semicircle, θ, of the impedance data corresponding to Fig. 1, as a function of the state-of-discharge; average values of five cells at each state-of-discharge (×). The data for a 6.8 mm × 2.6 mm (manufacturer A) cell are also shown (○, notice the scale on the right side).

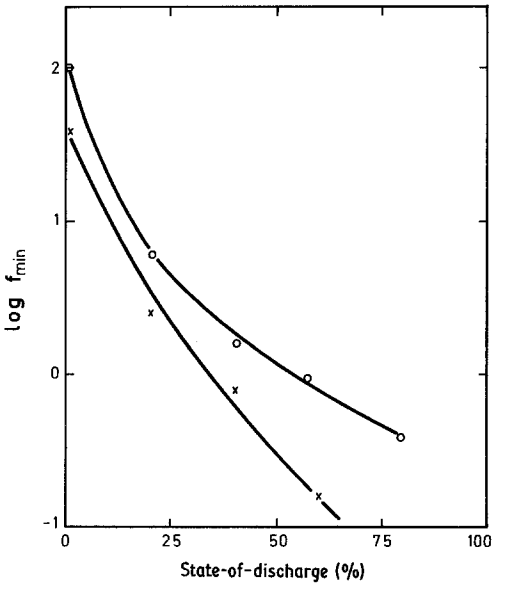

Fig. 3. Frequency at the minimum or inflexion point of the impedance data corresponding to Fig. 1 as a function of the state-of-discharge; average values of five cells at each state-of-discharge (×). The data for a 6.8 mm × 2.6 mm (manufacturer A) cell are also shown (○).

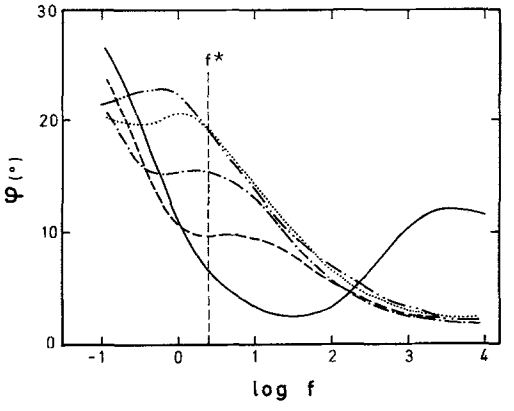

Fig. 4. Phase of the impedance data corresponding to Fig. 1 as a function the log of the frequency at 0 (——), 20 (– – –), 40 (–·–·–), 60 (····) and 80% state-of-discharge (–···–···–). The selection frequency is shown as $f^* = 2.5$ Hz.

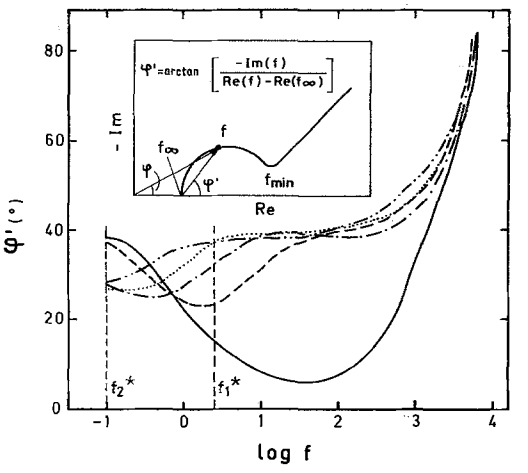

Fig. 5. Corrected phase angle φ' of the impedance data corresponding to Fig. 1 as a function of log f at 0 (——), 20 (– – –), 40 (–·–), 60 (····) and 80% state-of-discharge (–···–···–). Two possible selection frequencies are shown as $f_1^* = 2$ Hz and $f_2^* = 0.1$ Hz. The insert shows the definition of the phase φ'. Experimentally f_∞ is taken at 10 kHz.

A fixed frequency, f_{min}, therefore cannot be used to measure the real component. The frequency should be swept down to the minimum or inflexion point to determine f_{min} accurately.

The partial Bode representation is shown in Fig. 4 for five states-of-discharge. Both module and argument of the impedance were investigated but only the latter gives interesting results. The maximum and minimum of the complex impedance plot for the undischarged cell are seen in Fig. 4 as a well-defined maximum and minimum of the phase angle φ as a function of log f. For the partly discharged cells the two extrema were either ill-defined or the plot exhibited only an inflexion point which would be difficult to detect electronically.

One way to improve the resolution of the phase angle was to use a corrected phase angle, φ', calculated by subtracting the ohmic resistance from the real component as shown in the insert of Fig. 5. The advantage here was to eliminate the purely ohmic contribution and thus increase the value of the angle. The corrected phase angle, φ', is shown in Fig. 5 as a function of log f. In this representation the maximum of the complex impedance plot cannot be seen as a maximum, while the minimum at the intersection of the semicircle and straight line can always be seen as a minimum. The experimental points at frequencies between about 10 Hz and 10 kHz for states-of-discharge ≧ 20% were far from an ideal semicircle line. In fact they were closer to a linear plot with deviations large enough to create shallow minimum or inflexion points in the high-frequency region which are difficult to differentiate electronically from the real minimum occurring at a lower frequency. Figs. 6 and 7 give an example of the phase φ and corrected phase angle φ' vs log f curves exhibiting two well-defined minima, at least at some of the states-of-discharge investigated. These two minima are originating from

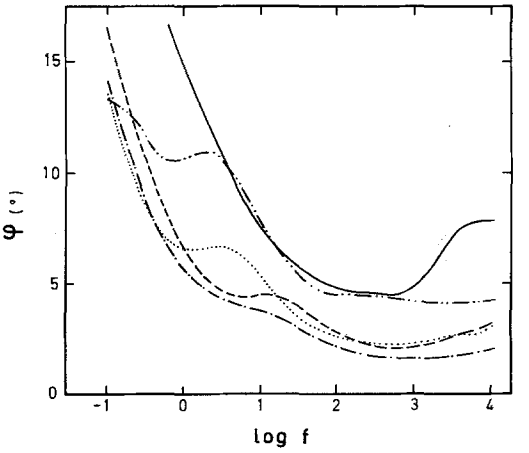

Fig. 6. Phase of the impedance for a 7.8 mm × 2.1 mm (manufacturer E) low drain cell as a function of log f at 0 (——), 6 (– – –), 40 (–·–·–), 60 (·····) and 74% state-of-discharge (–···–···–).

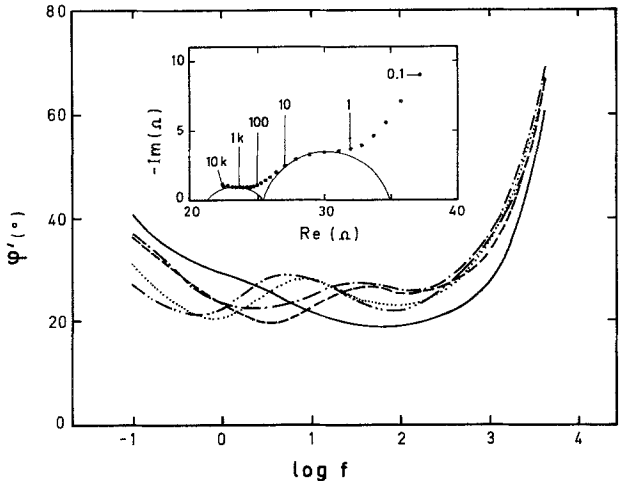

Fig. 7. Corrected phase angle φ' as a function of $\log f$ for the same cell as in Fig. 6. The insert shows the complex plane impedance data at 60% state-of-discharge.

the occurrence of two non-ideal semicircles at high frequencies as seen in the insert of Fig. 7.

The simplest selection criterion which could lead to the fastest state-of-discharge measurement was found to be related to the phase φ or the corrected phase φ' at an appropriate frequency f^*. Fig. 8 gives plots of φ and φ' as a function of the state-of-discharge at $f^* = 2.5$ Hz for the same cell as in Figs. 1–5. For this particular type of cell, the angle of selection φ^* or φ'^* and the variation of this angle with discharge were about twice as much for φ' as for φ. This could be experimentally an advantage for the corrected phase method since the accuracy should be better and the instrumentation simpler and cheaper.

Usually the optimum selection was carried out at the same frequency for both φ and φ'

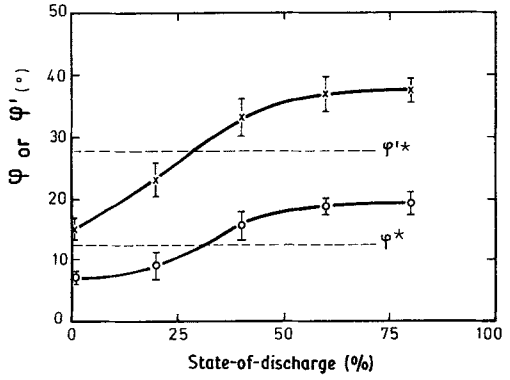

Fig. 8. Phase φ(○) and corrected phase φ'(×) of the impedance data corresponding to Fig. 1 at $f^* = 2.5$ Hz as a function of state-of-discharge; average values of five cells at each state-of-discharge.

(see Fig. 8). For some types of cells, one criterion or the other, or exceptionally both, did not permit a cell selection at a frequency higher than 0.1 Hz. For others (as shown in Fig. 5) the selection could be made at more than one frequency, i.e. at $f_1^* = 2$ Hz and $f_2^* = 0.1$ Hz. For practical reasons the highest frequency was normally preferred.

All the cells investigated did not exhibit the same behaviour as those shown in Figs. 1–5 and 8. The complex impedance plot of the undischarged cell was sometimes found to be quite featureless (Fig. 9). In that case, θ and f_{min} were not easily defined and the corrected phase angle was within the experimental scatter, the same at all the states-of-discharge investigated and at all the frequencies between 0.1 Hz and 10 kHz (Fig. 10). The only parameter which could be used as a state-of-discharge indicator was found to be the phase angle whose variation with $\log f$ is shown in Fig. 11. The dependence of the phase angle φ on the state-of-discharge at $f^* = 6.3$ Hz is just large enough to select the cells at a state-of-discharge $\leqq 40\%$ of which $\varphi < 6 \pm 0.2\%$ (see Fig. 10). This example is a particular case in which the selection is made possible by the regular decrease of the internal resistance of the cell with the state-of-discharge (see Fig. 9) which shifts the φ vs state-of-discharge curves towards the higher values of φ as the state-of-discharge increases. In fact, the selection here is based on a change of the resistance with state-of-discharge and not a variation of the characteristics of the electrode interfaces. For this particular type of cells the use of the internal

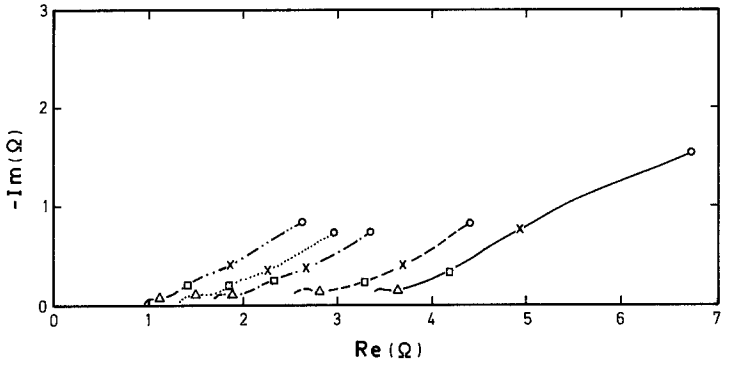

Fig. 9. Impedance data for a 9.5 mm × 2.1 mm (manufacturer C) low drain cell at 0 (———), 20 (– – –), 40 (–·–·–), 60 (·····) and 80% state-of-discharge (–···–···–) at $i_{dc} = 0$. (△) 1 kHz, (□) 10 Hz, (X) 1 Hz, (○) 0.1 Hz.

resistance as a state-of-discharge indicator would be as efficient as the phase angle.

Another difficulty may arise from the discrepancy between the behaviour of the undischarged and partly discharged cells as seen in Fig. 12. Here the only frequency range in which a selection could be made is below 10 Hz. Unfortunately, at the latter frequencies the undischarged cells cannot be differentiated from the ones with a high state-of-discharge. The same trend occurred in the φ' vs $\log f$ representation. The difficulty arose from a significant change of the impedance plot between the undischarged and partly discharged cells as seen in the insert of Fig. 12. Sharp variations between the frequency response of the undischarged and partly discharged cells were sometimes seen after only one per cent capacity had been withdrawn as seen in Fig. 13. In the latter case, however, there was no crossing of the low and high state-of-discharge values and a good selection could be made at $f^* = 10$ Hz. It is worth noting that in both Figs. 12 and 13 the value f_{min} decreased regularly with discharge.

Some measurements were also carried out as a function of the dc current level to investigate whether a more suitable state-of-discharge indicator could be found. Typical impedance data are shown in Figs. 14 and 15 in the undischarged state and at 60% state-of-discharge for the same type of cell as in Figs. 1–5 and 8. As the dc current increased, the low frequency straight line of the undischarged cell became increasingly curved towards the real axis of the complex plane representation. In the example of Fig. 14, the diameter of the high-frequency semicircle decreased with increasing current level. For some

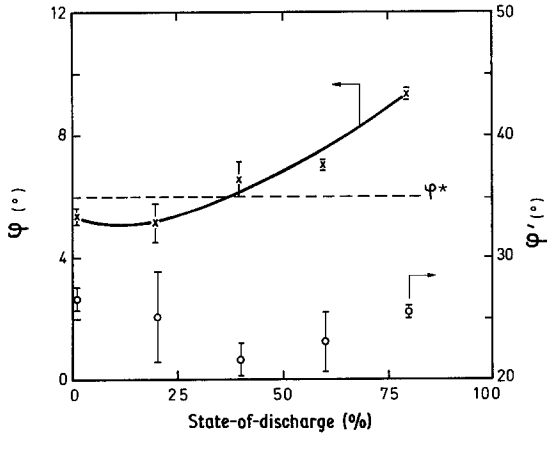

Fig. 10. Phase φ at $f^* = 6.3$ Hz(X) and corrected phase φ' at $f^* = 0.25$ Hz (○) of the impedance data corresponding to Fig. 9 as a function of state-of-discharge; average values of five cells at each state-of-discharge.

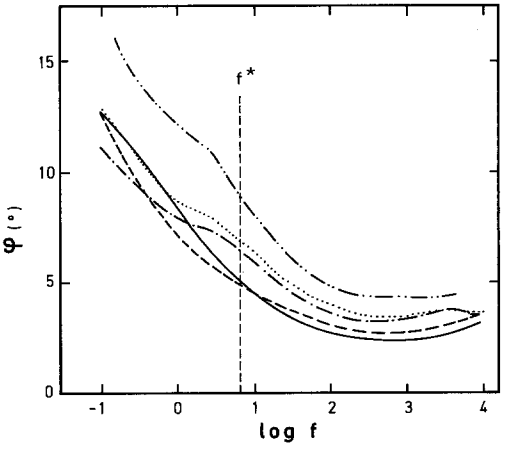

Fig. 11. Phase of the impedance data corresponding to Fig. 9 as a function of $\log f$ at 0 (———), 20 (– – –), 40 (–·–·–), 60 (·····) and 80% state-of-discharge (–···–···–). The selecting frequency is shown as $f^* = 6.3$ Hz.

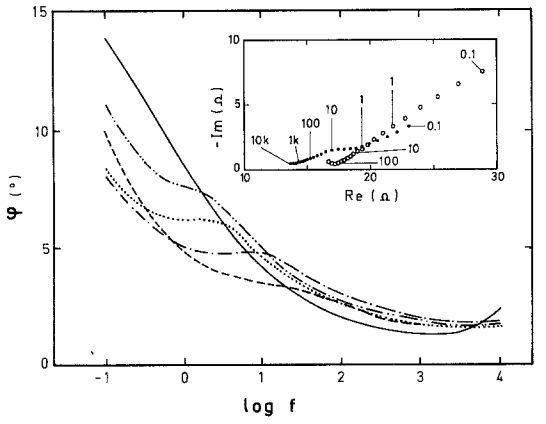

Fig. 12. Phase of the impedance data of a 11.6 mm × 4.2 mm (manufacturer F) low drain cell as a function of log f at 0 (———), 10 (– – – –), 21 (–·–·–), 64 (·····) and 85% state-of-discharge (–··–··–). The insert shows the complex plane impedance data at 0 (○) and 21% state-of-discharge (●).

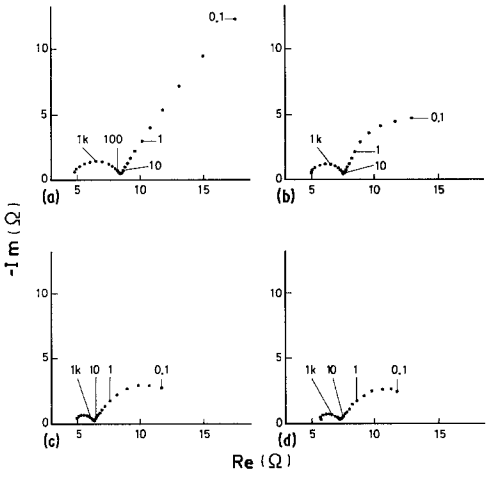

Fig. 14. Impedance data for the same type of cell as in Fig. 1 in the undischarged state measured at several dc current levels: (a) 0 μA, (b) 0.5 mA, (c) 1.0 mA and (d) 1.5 mA.

other cells the high-frequency contribution was not significantly changed by the dc current level (see Fig. 16). In contrast, the impedance data of the partly discharged cell changed only slightly with the level of the dc current (see Fig. 15).

It should be pointed out that the dc current must be relatively large to change significantly the impedance response obtained under zero dc current conditions. The influence was mainly seen at low frequency and at low state-of-discharge values. A state-of-discharge indicator could use the decrease of the imaginary component of the impedance from zero dc current to about 1 mA (for the cell shown in Figs. 14–16). However, the measurement at low frequency would require a long time. In addition, some charge would be withdrawn during the test. The determination of the state-of-discharge using a dc current drain is therefore of limited interest for a measurement device for rapid determination.

Calibrations were performed for 40 types of cells: 8 high drain and 32 low drain. The results of the calibration measurements are shown in Tables 2 and 3 for the two selection criteria φ

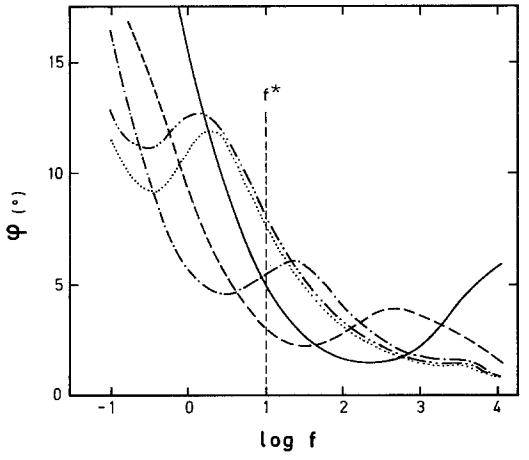

Fig. 13. Phase of the impedance data of a 7.9 mm × 3.1 mm (manufacturer A) low drain cell as a function of log f at 0 (———), 1 (– – – –), 20 (–·–·–), 60 (·····) and 80% state-of-discharge (–··–··–).

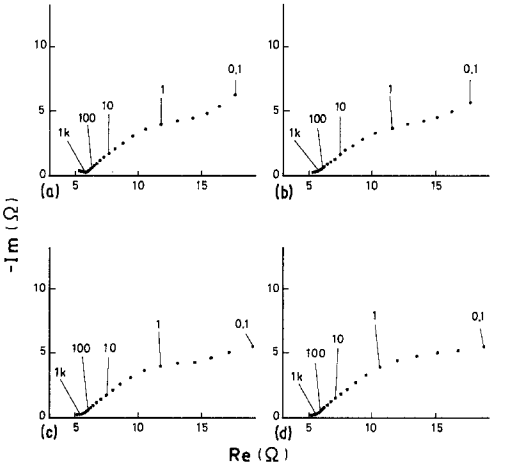

Fig. 15. Same as in Fig. 14 for a cell at 60% state-of-discharge.

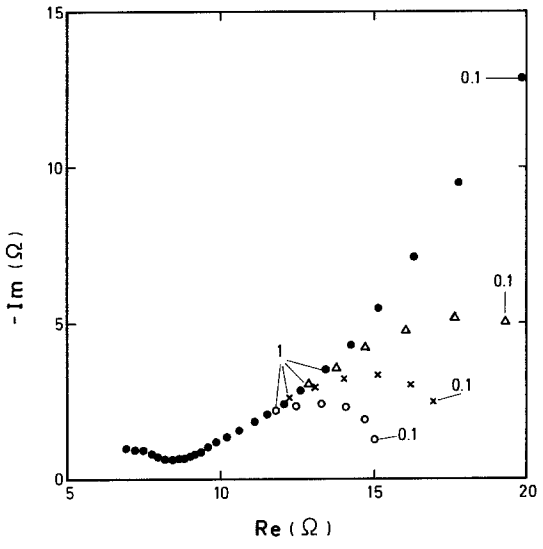

Fig. 16. Impedance data for an undischarged 9.5 mm × 2.1 mm (manufacturer E) low drain cell measured at $i_{dc} = 0$ μA (●), 0.5 mA (△), 1.0 mA (×) and 1.5 mA (○).

and φ'. Table 4 summarizes the results. All the types of cells have been characterized with the corrected phase angle φ', while only 25 types were measured using the phase angle φ. For eight types, noted as NOK in Tables 2–4, the selection was judged unsatisfactory. It is interesting to note that these eight types are not the same for the φ or φ' method. It follows that if the two methods are considered, only four types out of 25 could not be selected satisfactorily. In the latter case, the electrical characteristics of the cells are too scattered or there is too much similarity between the φ and φ' values in the undischarged state and at very high states-of-discharge in the appropriate frequency range.

A good state-of-discharge tester should give a rapid result which implies a high measurement frequency. A distinction has been made in Table 4 between the cell types which can be selected at

Table 2. Selection parameters for cells investigated using the phase angle φ as state-of-discharge indicator. The parameters are given in the following order: manufacturer/f (Hz)/$\varphi^*_{selection}$(°)/state-of-discharge$_{selection}$ (%). Unless otherwise noted the value $\varphi < \varphi^*$ selection corresponds to a state-of-discharge value < state-of-discharge$_{selection}$.*

(a) Low drain cells

Height (mm)	*Diameter (mm)*			
	6.8	*7.9*	*9.5*	*11.6*
1.1		A, NOK		
1.6	A/2/12/30	A/25/6/20	A, NOK	
2.1	A/6/9/40	A/6/9/20	A/4/9.2/40	A/2.5/12.4/40
	B, NOK	B, NOK		
		C/6.3/7/40	C/6.3/5.8/40	
		E, NOK		
2.6	A/6/7.5/40	A/4/9/40	A, NOK	
		B, NOK		
	C/6.3/9.4/40			
3.1		A/10/6.6/20		
3.6		A/1.6/7.4/30		
4.2				F, NOK

(b) High drain cells

Height (mm)	*Diameter (mm)*			
	6.8	*7.9*	*9.5*	*11.6*
2.6		A/0.16/> 14/< 30		
		C/15.9/5/40		
3.6		F/10/6.7/20		
5.4				F/0.25/> 12/< 20

Table 3. Selection parameters for cells investigated using the corrected phase angle φ' as state-of-discharge indicator. The parameters are given in the following order: Manufacturer/f (Hz)/$\varphi^*_{selection}$ (°)/state-of-discharge$_{selection}$ (%). Unless otherwise noted the value $\varphi' < \varphi'^*_{selection}$ corresponds to a state-of-discharge value < state-of-discharge$_{selection}$. (a) low drain cells*

Height (mm)	*Diameter (mm)*			
	6.8	*7.9*	*9.5*	*11.6*
1.1	A/10/30/30	A/1/32/40		
1.4		A/10/38/40		
1.6	A/6/32/40	A/16/29/40	A/16/29/20	
	B/0.4/> 26/< 20	B/4/27/20		
2.1	A/10/31/20	A/6/27/30	A/4/28/40	A/2.5/29/20
	B, NOK	B, NOK		B/0.4/> 28/< 20
	C/0.16/> 28/< 40	C, NOK	C, NOK	C/2.5/21/40
	E/0.16/> 26/< 20	E/0.16/> 31/< 40	E/25/21/20	
2.6	A/10/27/30	A/6/30/30	A/10/34/20	
		B, NOK		
	C/1.6/26/40			
		E/0.16/> 30/< 40		
3.1		A/16/35/20		A/4/25/40
3.6		A/4/29/40		
4.2				F, NOK

a frequency > 1 Hz and those which require a lower frequency. Only three out of 25 types need a measuring frequency < 1 Hz. It is worth pointing out that in the selection made at $f^* > 1$ Hz, the cells which have a state-of-discharge < 40% have a φ or φ' value smaller than the selection value φ^*, while for a frequency < 1 Hz the value of φ or φ' is larger than φ^* at a state-of-discharge < 40%.

4. Discussion

4.1. *Ideal state-of-discharge indicator: detection of a critical frequency*

The aim of the present study was to find a universal method suitable for all types of cells, independent of sizes, manufacturers and lot number. The search for an intensive parameter, i.e. independent of the amount of active material was therefore mandatory for both the measuring and the selecting parameters. The voltage at the two terminals is an intensive parameter and does not reflect the amount of active material, for example, while the current is an extensive parameter. The galvanostatic method recently discussed fails to achieve this goal since the current level is a function of the nominal capacity of the cells [1].

In the present study, the small ac signal superimposed on the cell voltage and the frequency at the maximum of the semicircle or at the minimum of the impedance spectra are both intensive

Table 3. Selection parameters for cells investigated using the corrected phase angle φ' as state-of-discharge indicator. The parameters are given in the following order: Manufacturer/f (Hz)/$\varphi^*_{selection}$ (°)/state-of-discharge$_{selection}$ (%). Unless otherwise noted the value $\varphi' < \varphi'^*_{selection}$ corresponds to a state-of-discharge value < state-of-discharges$_{selection}$. (b) High drain cells*

Height (mm)	*Diameter (mm)*			
	6.8	*7.9*	*9.6*	*11.6*
2.1		E/0.16/> 35/< 20		F, NOK
2.6		A/0.4/> 27/< 40		
		C, NOK		
		E/0.16/> 33/< 40	E/16/23/40	
3.6		F/0.25/> 24/< 20		
				F/0.4/> 20/< 20

Table 4. Summary of results of the measuring parameters for selection at a state-of-discharge ≦ 40%

Selection criteria	*Total number of types*	*Number of types* $f^* \geqq 1$ *Hz* φ' *or* $\varphi' < \varphi^*$	*Number of types* $f^* < 1$ *Hz* φ *or* $\varphi' > \varphi^*$	*Number of types NOK*
φ	25	15	2	8
φ'	25	15	3	7
	40	21	11	8
φ or φ'	25	18	3	4

parameters. On the contrary, the values θ and the phase angle φ and φ' are extensive parameters. Thus the most attractive method involves the detection of the relaxation frequency or f_{min}. Unfortunately, the exploitation of the data is ambiguous due to the non-ideal shape of the complex impedance plot. The first difficulty arises from the fact that the impedance plot seldom corresponds to a high-frequency semicircle and a straight line of 45° slope at low frequency as shown in Fig. 1a. This almost ideal behaviour gives a phase vs frequency plot (Fig. 4) from which the relaxation frequency and f_{min} can easily be determined. By contrast, in Fig. 1b–d the relaxation frequency is not clearly defined and the minimum has become an inflexion point. Therefore, only the values f_{min} can be extracted from Figs. 4 and 5. Irregularities in the impedance plot create secondary minima which cannot be easily differentiated electronically from the main minimum corresponding to f_{min} (Figs. 6 and 7). If the selection based on the f_{min} value was unambiguous electronically, an f_{min} value of > 1–10 Hz would correspond to a state-of-discharge $< 30\%$.

4.2. *Determination of the diameter of the high-frequency semicircle*

Since a state-of-discharge indicator based on an intensive parameter is not practical, attempts have been made to exploit other parameters investigated in the present study. The determination of the value θ also relies on the relaxation frequency or f_{min}. The basic limitations described for the determination of f_{min} are also valid here. In addition, the determination of f_{min} or θ would require a scanning of the frequency starting from the higher value down to about 1 Hz with a number of frequencies large enough to permit a precise determination. Thus the measurement time would depend on the number of cycles over which integration occurs, the number of points and the lowest frequency. As an example, 10 or 100 s are required for 1 or 10 cycles, respectively, and 5 points per decade of frequency from 10^4 down to 1 Hz.

4.3. *State-of-discharge indicator based on φ or φ'*

The most practical test based on the exploitation of the impedance data was found to be the determination of either the phase of the impedance φ, or the corrected phase φ'. The proposed test is a 'go/no go' indication based on one measurement carried out at an appropriate frequency for φ or two measurements for φ' performed at an appropriate frequency (usually the same as before) and at the highest frequency, e.g. 10 kHz. The main characteristics of the method will be compared below with the ideal requirements.

1. The selection should be made at a state-of-discharge ≦ 30%. Cut-off values between 20 and 40% state-of-discharge are usually obtained.
2. The charge withdrawn during the measurement should be as small as possible. There is no significant charge removed during the test since the perturbation is an ac signal superimposed on the open-circuit voltage.
3. The time of the test should be as short as possible. Times between 1 and 100 s are necessary depending on the characteristics of the cell, i.e. the frequency of the measurement.
4. The selection parameter should be independent of the parameter of the measurement. The critical values of the phase φ and the corrected phase φ' depend on the frequency of the measurement. An appropriate critical value of φ or φ' should therefore by used at a given frequency.

5. The selection and measuring parameters should be independent of the dimensions and manufacturer of the cell. A calibration is necessary for each cell dimension and each manufacturer. For example, for low drain cells from manufacturer A, $\varphi < 6–12°$ corresponds to a state-of-discharge < 20–40% at $f^* = 1–25$ Hz and $\varphi' < 25–33°$ corresponds to a state-of-discharge < 20–40% at $f^* = 1–16$ Hz, while for low drain cells from manufacturer E, $\varphi' > 26–31°$ corresponds to a state-of-discharge < 20–40% at $f^* = 0.16$ Hz.
6. The response should be independent of the history of the cell. This parameter has not been systematically investigated.
7. The principle of the method should be as simple as possible to permit the fabrication of a low cost device. The measurement of the phase φ requires a phase meter while the determination of the corrected phase φ' needs more complex circuitry with a memory to store the value $\mathrm{Re}_{(f\infty)}$ and a calculator to determine the real and imaginary values of the impedance at f^* (see Fig. 5). Laboratory equipment similar to that used in the present study including an FRA, electrochemical interface, calculator and plotter, are necessary to make the required calibrations.

The main disadvantages of the proposed method are:

(a) the need for a calibration for each type of cells and each manufacturer. The equipment needed to perform the calibration is quite expensive.
(b) the lack of universality. Four types of cells out of 25 investigated with both φ or φ' criteria could not be selected successfully due to: i. too large a dispersion of the impedance response occurring in small newly developed types; and ii. the similarity of both the φ and φ' values in the undischarged state and at very high state-of-discharge in the appropriate frequency range.

The latter difficulty arises from the different frequency response between the undischarged and the partly discharged cells (see, e.g. Figs. 4, 5 and 12). When this change occurs at high frequencies (Figs. 4 and 5), it does no harm to the state-of-discharge determination, while at low frequencies it may lead to a crossing of the low and high state-of-discharge responses which prevents the measurement of the state-of-discharge.

Finally, the proposed method fails to predict a cell failure due to an internal short circuit occurring after the test.

Before the change in frequency response can be ascribed to any particular element it is crucial to know the impedance behaviour of each electrode. The results of such a study will be presented in Part III of this series.

4.4. *Comparison with other zinc cells*

Attempts to develop a device for the estimation of the remaining capacity in primary Zn cells in the range 0–10% of the nominal capacity (100–90% of the fully-charged state) has been reported recently, using the impedance method for Leclanché [2], alkaline Zn–MnO_2 [3–5] and Zn–HgO [6] cells. The cells investigated were much larger than those used in the present study, i.e. 26 mm diameter × 50 mm height for the Leclanché and 14.5 mm diameter × 50 mm height for the alkaline Zn–MnO_2 and Zn–HgO cells.

A relatively simple correlation was found for the Zn–HgO cell between the diameter of the semicircle θ and the discharge, D, between 100 and 90% of the full-rated capacity. Practically, the test may be carried out by measuring the difference between the resistances at frequencies of 10 kHz and 31.2 Hz [6, 7]. With the Leclanché cell, it was found that the real impedance component at 31.2 Hz was a linear function of the state-of-discharge and fell from a value of about 2 Ω at 0% to 1 Ω at 10% [2]. The alkaline Zn–MnO_2 cell has proved to be a very difficult system for state-of-discharge estimation [3]. No correlation based on simple one- or two-frequency measurements could be found [3–5]. However, simple test conditions may be specified for each type of cell which will guarantee that a cell is less than 10% discharged. For the cell type investigated by Karunathilaka *et al.* [3], the resistance at a frequency of 0.5 Hz should not exceed 0.30 Ω coupled with an open circuit voltage of at least 1.48 V.

Table 5. Comparison of results obtained with the impedance and galvanostatic methods on the same types of button cells

Number of types	*Method*					
	Impedance (φ or φ')	*Galvanostatic* [$-\Delta E/\Delta t$ (2–10 s) *or* $-\Delta E/\Delta t$ (10–30 s)]	*Impedance or galvanostatic*	*Impedance* (φ *or* φ')	*Galvanostatic* [$-\Delta E/\Delta t$ (2–10 s) *or* $-\Delta E/\Delta t$ (10–30 s)]	*Impedance or galvanostatic*
Total	25	25	25	38	38	38
OK	21	22	25	34	32	38
NOK	4	3	0	4	6	0

4.5. *Comparison of the impedance method with a galvanostatic method*

Changes in the characteristics of the electrode interfaces as a function of the state-of-discharge are used in the impedance method. At frequencies larger than about 1 Hz these changes involve contributions from charge transfer, adsorption and to a small extent, diffusion. At frequencies lower than 1 Hz the contribution from diffusion is significantly increased. One advantage of the impedance method is that there is no dc current withdrawn from the cell and consequently, the test is entirely nondestructive and no significant amount of charge is removed. Another method has been investigated in which the contribution from diffusion is measured under galvanostatic control [1]. Here of course, a certain amount of charge is withdrawn from the cell, typically 0.1% of the nominal capacity.

A comparison of the results obtained with both methods on either 25 or 38 different types of button cells from five manufacturers is summarized in Table 5. The 25 types of cells are the same as those investigated in Table 4. In addition some other types have also been studied but not necessarily with both φ and φ' methods. The total number of types for which both the galvanostatic and impedance methods have been investigated is 38. Four types could not be selected at an appropriate state-of-discharge level using the impedance method and six using the galvanostatic method. If one test or the other is considered, all the types investigated could be selected between 20 and 50% state-of-discharge. The two methods are therefore found to be complementary, since the types of cells which could not be selected effectively with one method could be handled successfully with the other.

The main characteristics of both methods are shown in Table 6. The selecting level is somewhat lower with the impedance method. This is a significant advantage for a 'go/no go' test. The time of measurement of the impedance method depends on the frequency at which the measurement is carried out. A high frequency is always more suitable. The charge withdrawn is much higher in the case of the galvanostatic method while the success ratio, i.e. the number of types which could be selected with respect to the total number of types investigated with both methods, is slightly higher for the impedance method.

Acknowledgements

The author is pleased to thank F. Züllig for his skillful assistance in the experimental work and in the analysis of the data and C. E. Leuenberger for helpful discussions.

Table 6. Main characteristics of the impedance and galvanostatic methods

Characteristic	*Impedance method*	*Galvanostatic method*
Selecting level (% state-of-discharge)	20–40	30–50
Time of measurement (s)	1–100	10–30
Charge withdrawn (% C_{nom})	~ 0	0.1–0.5
Success ratio for 38 types (%)	89	84

References

[1] J. P. Randin, *J. Appl. Electrochem.* **15** (1985) 293.
[2] S. A. G. R. Karunathilaka, N. A. Hampson, R. Leek and T. J. Sinclair, *ibid.* **10** (1980) 799.
[3] *Idem, ibid.* **11** (1981) 365.
[4] M. Hughes, S. A. G. R. Karunathilaka, N. A. Hampson and T. J. Sinclair, *ibid.* **13** (1983) 217.
[5] M. L. Gopikanth and S. Sathynarayana, *ibid.* **9** (1979) 581.
[6] S. A. G. R. Karunathilaka, N. A. Hampson, T. P. Haas, R. Leek and T. J. Sinclair, *ibid.* **11** (1981) 573.
[7] S. A. G. R. Karunathilaka, N. A. Hampson, M. Hughes, W. G. Marhsall, R. Leek and T. J. Sinclair, *ibid.* **13** (1983) 577.
[8] M. Keddam, Z. Stoynov and H. Takenouti, *ibid.* **7** (1977) 539.
[9] M. L. Gopikanth and S. Sathyanarayana, *ibid.* **9** (1969) 369.
[10] S. Sathyanarayana, S. Venugopalan, and M. L. Gopikanth, *ibid.* **9** (1979) 125.

Publisher's note

Part III will appear in the next issue.